Marine Pollution Bulletin 225 (2026) 119304

Contents lists available at ScienceDirect

Marine Pollution Bulletin

journal homepage: www.elsevier.com/locate/marpolbul

Triple threat: Ocean acidification, warming, and hyposalinity synergistically weaken shell integrity in a Mediterranean calcifying mollusk

Arianna Mancuso [a,b,*,1], Francesca Giovanna Bardone [a,**,1], Chiara Marchini [a], Matilde Gironi [a], Anna Chiara Dalpozzo [a], Teresa Sani [a,b,c], Federico Girolametti [d], Anna Annibaldi [b,d], Francisco Arenas [e,**], Giuseppe Falini [b,f,2], Stefano Goffredo [a,b,2]

[a] Marine Science Group, Department of Biological, Geological and Environmental Sciences, University of Bologna, Via F. Selmi 3, 40126, Bologna, Italy
[b] Fano Marine Center, The Inter-Institute Center for Research on Marine Biodiversity, Resources and Biotechnologies, Viale Adriatico 1/N, 61032, Fano, Italy
[c] Institute for Biological Resources and Marine Biotechnologies, National Research Council (IRBIM, CNR), Largo Fiera della Pesca 2, 60125, Ancona, Italy
[d] Department of Life and Environmental Sciences, University Politecnica delle Marche, Via Brecce Bianche, 60131, Ancona, AN, Italy
[e] Benthic Ecology and Environmental Solutions Team, CIIMAR, University of Porto, Terminal de Cruzeiros do Porto de Leixões, Avenida General Norton de Matos, S/N 4450-208, Matosinhos, Portugal
[f] Department of Chemistry "Giacomo Ciamician", University of Bologna, 40126, Bologna, Italy

ARTICLE INFO

Keywords:
Bivalve
Ocean acidification
Warming
Hyposalinity
Mediterranean Sea
Multi-stressors interaction
Calcification
Fragile shells

ABSTRACT

Anthropogenic climate change is rapidly altering marine environments primarily through ocean warming, acidification, and hyposalinity, posing significant challenges for marine calcifying organisms. This study investigated the short-term effects of these stressors on the Mediterranean bivalve *Chamelea gallina*, a key fishery species in the Adriatic Sea, by integrating skeletal, mechanical, and mineralogical responses. Adult clams of commercial size were exposed for 21 days to eight experimental treatments manipulating two levels of temperature (18 °C vs. 22 °C), pH (8.0 vs. 7.9), and salinity (35 vs. 32), chosen to reproduce near-future climate projections and the freshwater-driven variability typical of the Adriatic Sea. Despite the short exposure duration, the combined exposure to low pH, high temperature, and reduced salinity weakens the shell of *Chamelea gallina* at multiple levels, compromising shell integrity, by making shells less dense, more porous, more fragile, and more susceptible to fracture, and increasing mortality. Microstructural analysis revealed smaller aragonite crystallites and lower calcium content, indicative of early impairments in the calcification process. The study highlights the occurrence of synergistic effects among stressors and reveals the vulnerability of *Chamelea gallina* to near-future ocean conditions, with potential cascading consequences for ecosystem functioning and fishery sustainability, given the species' key ecological role and commercial relevance in the Adriatic Sea.

1. Introduction

Rising atmospheric CO_2 concentrations, now exceeding 420 ppm, a level unprecedented in at least three million years, are driving ocean warming (OW) and acidification (OA), as the ocean absorbs ~25–30% of anthropogenic CO_2 emissions (Jiang et al., 2023; Lan et al., 2023; Lee et al., 2023; Nakamura and Ishida, 2025). These changes affect seawater carbonate chemistry by decreasing pH and carbonate ion (CO_3^{2-}) availability (Doney et al., 2020; Feely et al., 2023, 2009). As a consequence the aragonite saturation state (Ω_A) is reduced, impairing the capacity of calcifying organisms to produce and maintain calcium carbonate ($CaCO_3$) structures (Fitzer et al., 2014; Ries et al., 2009; Waldbusser and Salisbury, 2014). Simultaneously, increased sea temperatures accelerate metabolic demands and can divert energy from shell calcification (Frieder et al., 2017a; Ivanina et al., 2013; Lannig et al., 2010; Matoo et al., 2021). Under elevated temperature and

* Correspondence to: A. Mancuso, Marine Science Group, Department of Biological, Geological and Environmental Sciences, University of Bologna, Via F. Selmi 3, 40126, Bologna, Italy.
** Corresponding authors.
E-mail addresses: arianna.mancuso2@unibo.it (A. Mancuso), francesca.bardone@unibo.it (F.G. Bardone), farenas@ciimar.up.pt (F. Arenas).
[1] These authors share first authorship.
[2] These authors (joint senior authors) have equal responsibility for study supervision.

https://doi.org/10.1016/j.marpolbul.2026.119304
Received 17 November 2025; Received in revised form 15 January 2026; Accepted 15 January 2026
Available online 23 January 2026
0025-326X/© 2026 The Authors. Published by Elsevier Ltd. This is an open access article under the CC BY license (http://creativecommons.org/licenses/by/4.0/).

reduced pH conditions, bivalves experience increased oxidative stress due to enhanced production of reactive oxygen species (ROS) (Freitas et al., 2017; Matozzo et al., 2013; Rahman et al., 2019). The activation of antioxidant defence systems, together with acid–base regulatory mechanisms, increases metabolic costs, leading to a reallocation of energy away from shell calcification (Matozzo et al., 2013; Rahman et al., 2019). Moreover, in shallow waters, extreme precipitation events and freshwater inputs cause hyposalinity, which reduces aragonite saturation state (Ω_A) through a dilution of calcium (Ca^{2+}) and carbonate (CO_3^{2-}) ion concentrations and a concurrent decrease in total alkalinity (Sanders et al., 2018; Siedlecki et al., 2017). Because Ω_A depends on the product of these ions relative to the solubility product, the influx of ion-poor freshwater directly lowers saturation levels, thereby exacerbating conditions unfavorable for calcium carbonate precipitation (Sanders et al., 2018; Siedlecki et al., 2017). Recent evidence indicates that, in addition to impairing calcification, warming, acidification, and hyposalinity also affect other physiological pathways in marine organisms. For example, in *Chlamys nobilis*, acidification induced intestinal dysbiosis, oxidative stress, and reduced filtration and oxygen consumption (Liu et al., 2026), while in *Etroplus suratensis*, combined warming and acidification depressed metabolism and growth and elevated oxidative stress and apoptosis (Mahapatra et al., 2025). Similarly, in oysters and mussels, multi-stressor exposure altered tissue-specific carbon allocation, cellular stress biomarkers, and metabolite profiles (Kılıç et al., 2026; Meng et al., 2026).

These stressors are particularly dynamic and impactful in coastal and estuarine systems, where environmental variability is high and climate-driven changes are intensified (Andersson et al., 2006; Harris et al., 2013; Lejeusne et al., 2010). In shallow Mediterranean estuarine settings, such as the Northern Adriatic, salinity can fluctuate widely (e.g., from 26 to 38) and Total Alkalinity (A_t) and Dissolved Inorganic Carbon (DIC) typically range between 2300 and 2700 μmol kg^{-1} and 2200–2600 μmol kg^{-1}, respectively (Cossarini et al., 2015; Giani et al., 2023; Urbini et al., 2020). Moreover, while stressors may occur in isolation, globally 97.7% of the ocean is currently affected by multiple stressors, with climate-related drivers (particularly ocean warming and acidification) representing the dominant forces of change, alongside fishing, land-based pressures, and other commercial activities (Halpern et al., 2019). For calcifying organisms like mollusks, which rely on calcium carbonate ($CaCO_3$) for shell formation (Lowenstam and Weiner, 1989), such multi-stressor environments impair calcification and shell integrity, threatening ecological and economic resilience (Doney et al., 2020; Feely et al., 2009; Fitzer et al., 2014; Zhao et al., 2017). However, responses vary among species and life stages, with organisms producing aragonite-based shells, generally being more vulnerable due to their higher solubility and energetic cost (Beniash et al., 2010; Doney et al., 2020). In previous studies acidification has been linked to decreased shell growth and altered crystal structure in adults of *Nucella lamellosa*, *Littorina littorea*, as well as in juveniles of *Strombus luhuanus* (Nienhuis et al., 2010; Ries et al., 2009; Shirayama and Thornton, 2005), while combined low pH and high temperature have significantly impaired net calcification and reduced calcium incorporation in adults of *Pinctada fucata* (Li et al., 2016). Ocean acidification can also weaken shell mechanical resistance to breakage and fracture toughness in species such as *Crassostrea virginica* (juvenile oysters) and *Mytilus edulis* (adult mussels) (Dickinson et al., 2012; Fitzer et al., 2015; Ivanina et al., 2013). Salinity fluctuations, often exacerbated by altered precipitation patterns and freshwater inflows, further modulate bivalve responses. Although some species tolerate hyposalinity via osmoconformation, studies reveal reduced shell growth, altered ultrastructure, and elevated mortality when low salinity is combined with thermal or acidification stress (Bae et al., 2021; Rato et al., 2022). Importantly, many of these effects were detected during short-term exposures, suggesting that rapid skeletal responses can occur well before long-term physiological or demographic consequences become apparent.

Chamelea gallina, a key commercial bivalve of the Adriatic Sea, represents a relevant model for studying calcification under multiple stressors. Most existing studies have focused on juveniles of this species (Sordo et al., 2024, 2021), whereas adults, due to their infaunal lifestyle, sediment dependence, and inability to be cultured, pose logistical challenges for long-term experimentation (Grazioli et al., 2022). This clam inhabits the fine well-sorted sand biocenosis, occupying a well-defined ecological niche in the Adriatic Sea, determined by precise chemical-physical conditions of both water and sediment (Grazioli et al., 2022). It supports a historically important fishery in the Adriatic Sea, with current annual landings of approximately 10,000 metric tons, worth around €51 million (Italian National Management Plan for hydraulic dredges, 2019). In recent years, its populations have faced mounting pressures from overexploitation, alien predators such as *Callinectes sapidus*, and climate-driven stressors (FAO, 2023). Moreover, the shell of *C. gallina* is primarily composed of aragonite (Ries et al., 2009), making this species particularly vulnerable to changes in seawater chemistry (Kroeker et al., 2013). Warmer southern sites in the Adriatic are associated with lighter, thinner, and more porous shells (Gizzi et al., 2016; Mancuso et al., 2019), while northern areas influenced by freshwater inputs and lower salinity exhibit reduced calcification (Cheli et al., 2025; Mancuso et al., 2019). Water temperature and salinity thus emerge as key modulators of shell formation, acting on both the energetic and physicochemical fronts. However, the effects of ocean acidification and the interplay of OA, OW, and salinity changes on adult *C. gallina* remains unexplored, despite its ecological and commercial significance (Grazioli et al., 2022; Romanelli et al., 2009).

To address this gap, we conducted a controlled short-term mesocosm experiment to assess the individual and combined effects of lowered pH, elevated temperature, and reduced salinity on adult *C. gallina*, focusing on multiple parameters on diverse dimensional scales, from skeletal and mechanical properties to structural and mineralogical composition. By integrating multi-scale analyses, this study provides novel insight into the early responses and potential vulnerabilities of *C. gallina* under projected climate change conditions in coastal Mediterranean ecosystems.

2. Materials and methods

2.1. Experimental set-up and treatments

The experiment was conducted in a temperature-controlled room, by means of a semi-continuous flow-through seawater system made up of 24 mesocosms, each containing 60 l of seawater and 80 clams (Fig. 1, see Supplementary Information for more details). Before the tests began, a four-day acclimatization period in the mesocosms was provided. Clams were fed daily, ad libitum, with the microalgae *Isochrysis galbana* during both the acclimatization and experimental periods.

This study considered three environmental parameters, namely temperature, pH, and salinity, under both control and changing conditions (Fig. 1). Control values (18 °C, pH 8.0, salinity 35) were selected to replicate the present-day conditions experienced by *C. gallina* in the Adriatic Sea. The temperature (22 °C) and pH (7.9) levels were set according to reflect CMIP6-class projections for the Mediterranean Sea under the intermediate SSP2–4.5 “middle-of-the-road” scenario. Under this scenario, model projections indicate basin-wide surface warming of roughly +1–3.5 °C and a mean surface pH decline of ~0.1–0.2 units by 2070–2100 relative to late-20th-century conditions, with the Mediterranean acting as a regional warming and acidification hot-spot compared to the global ocean (Kristiansen et al., 2024; Zittis et al., 2019). End-of-century pH values of ~7.7–7.8 projected under stronger acidification (−0.3 to −0.4) were not applied, as such extreme conditions can trigger severe acute stress responses and mortality in adult clams during the short-term 21-day experiment. Salinity (32) was manipulated to reflect the natural gradient of the Adriatic Sea, where freshwater discharge from large river systems, particularly the Po, periodically lowers coastal salinity. Although climate projections for the

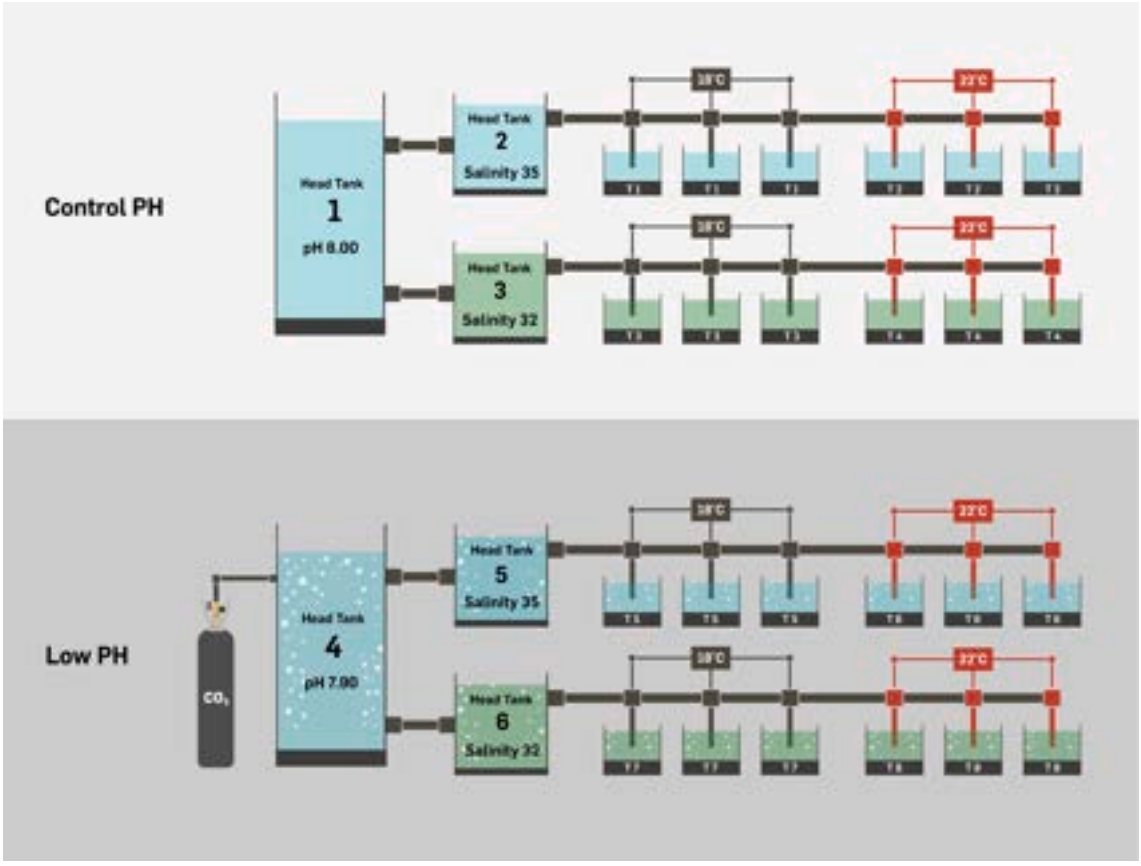

Fig. 1. Experimental set-up. The eight treatments are arranged in two groups: the four treatments in the top white box correspond to control pH conditions, while the four in the bottom grey bow, with CO_2 bubbling, represent reduced pH conditions. Seawater colors indicate salinity levels: light blue represents control salinity, while green represents reduced salinity. Temperature levels are shown in the small boxes above the treatments. Each mesocosm was equipped with an individual thermostat set to the target temperature for its specific treatment. (For interpretation of the references to colour in this figure legend, the reader is referred to the web version of this article.)

Adriatic Sea indicate a long-term tendency toward increased salinity due to reduced mean river discharge and enhanced evaporation (Ricci et al., 2024; Verri et al., 2024), climate change is also expected to increase the frequency and intensity of extreme precipitation and flood events. Observational studies show that these events with episodic freshwater pulses are already occurred, leading to short-term but pronounced reductions in coastal salinity, which are ecologically relevant stressors for benthic organisms (Krauzig et al., 2025 Preprint). The salinity treatment adopted in this study was designed to reflect these such episodic low-salinity events rather than long-term mean conditions. In total, eight experimental conditions were tested, resulting from different combinations of these three environmental parameters, with three mesocosm replicates for each (Fig. 1). The temperature, pH, and salinity from each experimental tank were measured twice daily (at 9 am and at 6 pm) using a digital temperature controller (INKBIRD ITC—1000F) and environmental probes (Multi meter HACH HQ40d). Total alkalinity (A_t) was determined colorimetrically following (Sarazin et al., 1999, see Supplementary Information for more details). A_t values, together with temperature, pH, and salinity, were used to calculate carbonate system parameters, using CO2SYS software.

For this study only clams of commercial size with minimum length of 22 mm were used, conforming to European normative which regulates *Chamelea gallina* minimum fishing size (22 mm, Commission Delegated Regulation (EU) No. 2237/2020). Specimens were sampled from fishermen off the coast of Cattolica in the Adriatic Sea using hydraulic dredges and transported to the CIIMAR, where the experiment was carried out.

2.2. Mortality and condition index

Mortality rate, defined as the percentage of dead individuals, was monitored daily throughout the 21-day experiment and determined by identifying dead individuals. At the end of experiment, surviving clams were used to assess the condition index by separating the soft internal tissue from the shells. Both shells and tissues were then dried at 50 °C for 72 h before being weighed. The Condition Index (CI) was calculated according to the following formula (Walne, 1976):

$$CI = \frac{\text{tissue dry mass (g)}}{\text{shell dry mass (g)}} \times 100$$

2.3. Shell biometric and skeletal parameters

Shell length (maximum distance on the anterior-posterior axis), height (maximum distance on the dorsal-ventral axis) and width (maximum distance on the lateral axis) were obtained with a caliper (± 0.05 mm). Shell thickness index (STI) was calculated (Freeman and Byers, 2006):

$$STI = \frac{1000 \times \text{Shell mass (g)}}{\left[\text{Length} \times \left(\text{Height}^2 + \text{Width}^2\right)^{0.5} \times \pi / 2\right]}$$

The Buoyant Weight (BW) techniques were used to estimate volume and shell density parameters, as in previous study on corals and marine mollusks (Caroselli et al., 2011; Gizzi et al., 2016; Mancuso et al., 2019). The BW measurement was performed with a density determination kit Ohaus Explorer Pro balance (±0.1 mg; Ohaus Corp., Pine Brook, NJ,

USA); measurments were repeated three times and the average was considered for statistical analysis. The following skeletal parameters were obtained:

I. Micro-density (g/cm^3) = the mass per unit volume of the material which composes the shell, excluding the volume of pores.
II. Apparent porosity (%) = the volume of the pores connected to the external surface.
III. Bulk density (g/cm^3) = the density of the valve, including the volume of the pores.

2.4. Shell resistance to compression

To assess shell resistance to mechanical stress, we measured maximum load (as a proxy for fracture load), and structural stiffness during compression tests using an Instron universal testing machine equipped with a 5 kN load cell, descending at a constant speed of 0.5 mm·min^{-1}. Compression tests were conducted on both dry and wet shells. Compression tests produced typical load–displacement curves consisting of an ascending and a descending phase. Based on the shape of the ascending curve, four main fracture patterns were identified (Cabral and Natal Jorge, 2007): Type I (continuous increase in load), Type II (1–2 minor peaks), Type III (multiple distinct peaks), and Type IV (one or several prominent peaks at high loads). The breaking force was identified from each loading curve and labeled as "Maximum load" (kN). Structural stiffness (kN mm^{-1}) was calculated as the slope of the load–displacement curve immediately before fracture, corresponding to the plastic deformation stage where the shell undergoes irreversible structural changes beyond its elastic limit.

2.5. Shell intra-skeletal content and mineral structure

The fragments resulting from the compression tests were cleaned to remove any trace of superficial organic residues by soaking them in a sodium hypochlorite solution 10 wt% for three days and rinsed with distilled water. Subsequently, the shell fragments were pulverized using a mechanical mortar to achieve a fine granulometry (less than 100 mm). To determine the organic matter content (OM), a Thermogravimetric analysis (TGA) was conducted using a SDT Q600 instrument. Approximately 12–14 mg of pulverized sample were placed in a ceramic crucible and subjected to heating from 30 °C to 900 °C at a rate of 10 °C·min^{-1} under a nitrogen flow of 100 ml·min^{-1}. The resulting thermograms were analyzed using TA Universal Analysis software. The content of structural water and OM was assessed by measuring the weight loss percentage between 150 °C and 500 °C, while $CaCO_3$ decarboxylation was observed between 500 and 900 °C.

X-Ray Diffraction (XRD) analyses were carried out using a Pan-Analytical X'Pert Pro diffractometer equipped with a multiarray X'Celerator detector. Cu Kα radiation was generated at 40 kV and 40 mA ($\lambda = 1.54056$ Å), with patterns collected within the 2θ range of 20 to 60°. The step size (Δ2θ) was set at 0.016°, and a counting time of 122 s was utilized. The resulting diffractograms were analyzed using Profex software to identify the crystalline phase (i.e., the specific mineral polymorph) and the crystallite size (i.e., the dimension of the crystallite within the crystal along one specific direction).

To further validate the characterization of the crystalline phase, Fourier Transform Infrared (FTIR) spectra analysis was conducted using a Thermo Scientific Nicolet iS10 FTIR spectrometer. Preparation of the disk sample involved creating a mixture of 100 mg, consisting of 98% KBr (Potassium Bromide) and 2% pulverized sample. From this mixture, 15 mg were utilized to form the disk by compressing it in a hand press. The spectra were acquired with a resolution of 4 cm^{-1} and 64 scans.

Shell calcium concentration was determined using inductively coupled plasma optical emission spectrometry (ICP-OES). Approximately 10 mg of dried and homogenized shell powder were mineralized using 8 ml of HNO_3 and 2 ml of H_2O_2 in a MARS-5 microwave digestion system (CEM, USA). Samples were then diluted 1:100 in 5% HNO_3 and analyzed using an Agilent 5800 ICP-OES, with a wavelength of 422.673 nm for Ca. Calibration was performed using five standards ranging from 1250 to 20,000 ppb Ca, with a rational fit calibration curve (correlation coefficient = 0.99965). Each sample was measured in triplicate using Ar as internal standard and DORM-5 as certified reference material (CRM). A limitation of the present study is that a single-step microwave-assisted digestion protocol was used, which efficiently dissolved the $CaCO_3$ matrix for the purposes of relative comparisons among treatments; however, sequential or double-digestion procedures may be required in other contexts to ensure complete solubilization of Ca-rich matrices. Additionally, DORM-5, a fish protein certified reference material, was used to assess analytical performance, as a matrix-matched certified reference material for carbonate shells was not available. While this may affect absolute accuracy, all samples were processed using the same digestion and analytical protocol, ensuring that relative comparisons among experimental treatments remain robust.

2.6. Statistical analyses

Data normality and homogeneity of the variances were assessed using Shapiro–Wilk and Levene's test, respectively. One-way ANOVA, followed by Tukey's post-hoc test, was used when parametric assumptions were met; otherwise, a non-parametric Kruskal-Wallis (K—W) test, followed by Dunn test's post-hoc with Holm correction, was applied. To assess the main and interactive effects of pH, temperature, and salinity on clam responses, linear mixed-effects models (LME) were fitted. When residuals did not satisfy model assumptions, a permutational multivariate analysis of variance (PERMANOVA, adonis2 function in vegan R package) was used instead. The analysis was based on a Euclidean distance matrix and 999 permutations. In addition, generalized linear models (GLMs) were used to explore the nature of the interactions (e.g., additive, synergistic, or antagonistic), complementing the results of LME or PERMANOVA. A Random Forest analysis was also performed to evaluate the relative importance of environmental predictors (temperature, salinity, pH, and aragonite saturation state). Highly collinear carbonate chemistry variables were excluded to prevent multicollinearity. Statistical analyses were conducted using R version 4.4.1 (R Core Team, 2024) within the RStudio environment (Posit team, 2025), including the packages ggplot2, ggpubr, car, vegan, nlme, and randomForest.

3. Results

3.1. Environmental parameters

The three environmental parameters (pH_T, temperature and salinity) did not differ among the three replica tanks in each treatment (K—W test, $p > 0.05$; Suppl. Table 1), nor among treatments with the same control and varying conditions (K—W test, $p > 0.05$). Therefore, values from the three replicate tanks were pooled to obtain a mean value for each treatment, which was then compared to the target value defined a priori for that specific experimental condition (Table 1). Total alkalinity and carbonate chemistry parameters were homogeneous among the three replica tanks within each treatment (K—W test, $p > 0.05$; Suppl. Table 2). The pCO_2, CO_3^{2-}, Ω_A and Ω_C, differed significantly among treatments (K—W test, $p \leq 0.05$, Table 2).

3.2. Mortality and condition index

Mortality rate differed among treatments (K—W test, $p < 0.01$) and post-hoc pairwise comparisons identified significant differences particularly between the control and the most stressful treatments ($T1_{control}$ – $T3_{\downarrow Sal}$ vs $T6_{\downarrow pH\ \uparrow Temp}$ - $T7_{\downarrow pH\ \downarrow Sal}$ - $T8_{\downarrow pH\ \uparrow Temp\ \downarrow Sal}$; Fig. 2). Random Forest analysis indicated that mortality was primarily associated with Ω_A, followed by temperature and pH (Random Forest, %IncMSE = 17.18,

Table 1
Seawater aquarium parameters measured for each treatment (T1 to T8; data from the three replicated tanks were pooled). Values are expressed as mean ± 95% confidence intervals. For temperature, pH_T, and salinity, $n = 114$ corresponds to the total number of measurements per treatment; for total alkalinity (A_T), $n = 57$ reflects fewer measurements due to a lower sampling frequency.

	pH_T				Temperature (°C)				Salinity				A_T (μmol kg^{-1})			
Treatment	Target	Observed			Target	Observed			Target	Observed			Observed			
T1 (control)	8.00	8.02	±	0.01	18.00	18.00	±	0.14	35.00	35.01	±	0.09	2565	±	106	
T2 (↑Temp)	8.00	8.02	±	0.01	22.00	21.93	±	0.11	35.00	35.22	±	0.09	2619	±	116	
T3 (↓Sal)	8.00	8.02	±	0.01	18.00	18.00	±	0.10	32.00	32.01	±	0.10	2621	±	73	
T4 (↑Temp ↓Sal)	8.00	8.02	±	0.01	22.00	21.96	±	0.09	32.00	32.16	±	0.10	2660	±	80	
T5 (↓pH)	7.90	7.89	±	0.01	18.00	18.02	±	0.11	35.00	35.09	±	0.09	2512	±	103	
T6 (↓pH ↑Temp)	7.90	7.89	±	0.01	22.00	22.00	±	0.11	35.00	35.24	±	0.08	2651	±	118	
T7 (↓pH ↓Sal)	7.90	7.89	±	0.01	18.00	18.02	±	0.09	32.00	32.03	±	0.10	2535	±	114	
T8 (↓pH ↑Temp ↓Sal)	7.90	7.89	±	0.01	22.00	21.93	±	0.10	32.00	32.14	±	0.12	2506	±	107	

Table 2
Carbonate chemistry parameters calculated for each treatment (T1 to T8; data from the three replicated tanks were pooled). Values are expressed as mean ± 95% confidence intervals; n = 57 represents the total number of measurements per treatment. Abbreviations: pCO_2, partial pressure of CO_2; DIC, dissolved inorganic carbon; HCO_3^-, bicarbonate ion concentration; CO_3^{2-}, carbonate ion concentration; Ω_A and Ω_C, aragonite/calcite saturation state. Different letters beside the values of pCO_2, CO_3^{2-}, Ω_A and Ω_C indicate post-hoc results (Dunn's test, $p \leq 0.05$), after significant results of Kruskal-Wallis test, reported in the last row as *p*-values.

Treatment	pCO_2 (μatm)			DIC (μmol kg^{-1})			HCO_3^- (μmol kg^{-1})			CO_3^{2-} (μmol kg^{-1})			Ω_A			Ω_C		
T1 (control)	464	±	23^a	2310	±	99	2105	±	91	190	±	8^{ac}	2.93	±	0.13^a	4.53	±	0.20^a
T2 (↑Temp)	476	±	22^a	2333	±	97	2094	±	95	218	±	11^a	3.41	±	0.17^b	5.22	±	0.26^b
T3 (↓Sal)	489	±	16^a	2385	±	68	2186	±	62	182	±	6^c	2.85	±	0.10^{ad}	4.44	±	0.15^a
T4 (↑Temp ↓Sal)	496	±	19^a	2387	±	73	2161	±	66	210	±	10^a	3.34	±	0.16^b	5.15	±	0.24^b
T5 (↓pH)	668	±	33^b	2333	±	97	2168	±	90	141	±	7^{df}	2.18	±	0.12^c	3.37	±	0.18^c
T6 (↓pH ↑Temp)	677	±	40^b	2426	±	112	2230	±	104	175	±	8^{ce}	2.74	±	0.13^a	4.20	±	0.20^a
T7 (↓pH ↓Sal)	691	±	38^b	2372	±	108	2214	±	101	134	±	8^{df}	2.10	±	0.12^{ce}	3.27	±	0.19^{ce}
T8 (↓pH ↑Temp ↓Sal)	633	±	41^b	2301	±	102	2120	±	95	161	±	8^e	2.55	±	0.13^{de}	3.93	±	0.20^{de}
Kruskal Wallis test	*0.000*			*0.651*			*0.376*			*0.000*			*0.000*			*0.000*		

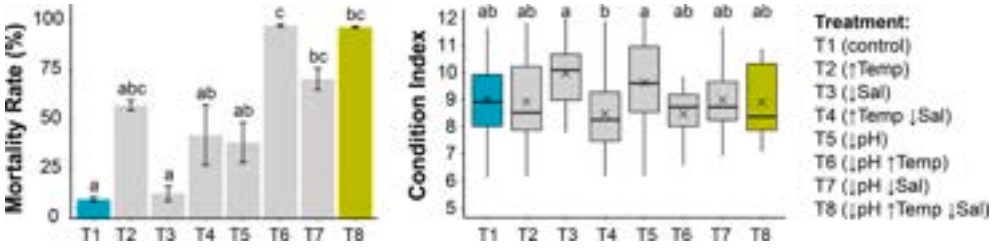

Fig. 2. Mean mortality rate (%) and condition index of clams across treatments. Bars of mortality rate represent mean values ± standard error. Crosses in the boxplot indicate the mean values of condition index. Different letters indicate post- hoc differences among treatments (Dunn's test and Tukey test, $p \leq 0.05$).

14.94 and 14.54, respectively). The highest mortality rate (around 97%) was observed in treatments with low pH and high temperature ($T6_{\downarrow pH\ \uparrow Temp}$ and $T8_{\downarrow pH\ \uparrow Temp\ \downarrow Sal}$), while mortality decreased by about 88–90% in the control (T1) and in the treatment where only salinity varied ($T3_{\downarrow Sal}$; Fig. 2). Mortality resulted affected by pH and temperature (PERMANOVA, $p = 0.001$), while their interaction was not significant. Salinity alone was not significant, although weak interactions were detected between salinity and the other factors (PERMANOVA, pH:S, $p = 0.049$ and T:S, $p = 0.020$). This suggests that acidification and warming independently drive mortality responses, while salinity has a minor modulatory role.

Few statistically significant differences in condition index were found among treatments (ANOVA and pairwise Tukey test, $p < 0.001$: $T3_{\downarrow Sal}$ vs $T4_{\uparrow Temp\ \downarrow Sal}$ and $T4_{\uparrow Temp\ \downarrow Sal}$ vs $T5_{\downarrow pH}$; Fig. 2), and no clear visual trend emerged due to high within-group variability.

3.3. Shell biometry and skeletal properties

Since all shell biometric parameters resulted homogeneous between the left and the right valves, mean values of the two valves were used in the analyses (Table 3). Shell biometric and skeletal parameters for each tank are shown in Supplementary information (Suppl. Table 3–4). Shell length, shell height, and shell width did not differ among treatments, whereas shell mass and shell thickness index (STI) did (K—W test, $p \leq 0.05$; Table 3). Post-hoc comparisons showed significant differences only for treatments $T4_{\uparrow Temp\ \downarrow Sal}$ and $T8_{\downarrow pH\ \uparrow Temp\ \downarrow Sal}$, with both shell mass and STI being lower under $T8_{\downarrow pH\ \uparrow Temp\ \downarrow Sal}$ (Dunn's test, $p \leq 0.05$; Table 3). Random Forest analysis identified pH as the main driver for mass and STI (%IncMSE = 9.07 and 11.29, respectively), followed by temperature (%IncMSE = 8.13 and 10.28, respectively). Neither shell mass nor STI were significantly affected by single environmental factors, except for a marginal effect of pH on thickness (PERMANOVA, $p = 0.041$). However, interactions between pH and temperature

Table 3
Biometric parameters of *Chamelea gallina* for each treatment (T1 to T8; data from the three replicated tanks were pooled). STI, Shell Thickness Index. Values are expressed as mean ± 95% confidence intervals; n = number of samples for each treatment. Different letters beside the values of Mass and STI indicate differences among treatments (Dunn's post-hoc test, p ≤ 0.05), after significant results of Kruskal-Wallis test, reported in the last row as *p*-values.

Treatment	*n*	Length (mm)			Width (mm)			Height (mm)			Mass (g)			STI		
T1 (control)	127	24.84	±	0.26	5.88	±	0.06	21.25	±	0.20	1.33	±	0.04^{ab}	2.23	±	0.04^{ab}
T2 (↑Temp)	53	24.93	±	0.46	5.89	±	0.10	21.39	±	0.32	1.34	±	0.07^{ab}	2.22	±	0.08^{ab}
T3 (↓Sal)	128	24.99	±	0.27	5.84	±	0.06	21.55	±	0.20	1.35	±	0.04^{ab}	2.24	±	0.04^{ab}
T4 (↑Temp ↓Sal)	71	25.45	±	0.38	5.99	±	0.09	21.67	±	0.30	1.41	±	0.06^{a}	2.30	±	0.07^{a}
T5 (↓pH)	95	24.85	±	0.27	5.91	±	0.07	21.53	±	0.22	1.33	±	0.04^{ab}	2.22	±	0.04^{ab}
T6 (↓pH ↑Temp)	25	24.67	±	0.52	5.87	±	0.13	21.45	±	0.41	1.30	±	0.07^{ab}	2.17	±	0.08^{ab}
T7 (↓pH ↓Sal)	54	24.81	±	0.53	5.92	±	0.11	21.49	±	0.34	1.34	±	0.07^{ab}	2.23	±	0.08^{ab}
T8 (↓pH ↑Temp ↓Sal)	27	24.65	±	0.63	5.85	±	0.15	21.40	±	0.43	1.25	±	0.08^{b}	2.09	±	0.09^{b}
Kruskal Wallis test		*0.068*			*0.396*			*0.054*			*0.036*			*0.029*		

(PERMANOVA, $p = 0.023$ for mass and $p = 0.012$ for STI), and between pH and salinity (PERMANOVA, $p = 0.007$ for mass and $p = 0.009$ for STI) significantly influenced both parameters.

Significant differences in skeletal properties were detected across treatments (K—W test, $p < 0.001$ for all variables; Fig. 3; Suppl. Table 5). Micro-density remained relatively stable, with minor variations across treatments, except for $T8_{\downarrow pH\ \uparrow Temp\ \downarrow Sal}$ (Fig. 3; Suppl. Table 5). In contrast, bulk density was more responsive to environmental change, with a 4.9% decrease in $T8_{\downarrow pH\ \uparrow Temp\ \downarrow Sal}$ (2.53 ± 0.04 g cm^{-3}) relative to the $T1_{control}$ (2.66 ± 0.01 g cm^{-3}; Dunn's test, $p < 0.001$; Fig. 3; Suppl. Table 5). Apparent porosity showed the clearest pattern, nearly doubling under $T8_{\downarrow pH\ \uparrow Temp\ \downarrow Sal}$ (10.13 ± 1.71%) compared to the $T1_{control}$ (5.27 ± 0.47%), with a + 92.1% increase (Dunn's test, $p < 0.001$; Fig. 3; Suppl. Table 5). Porosity and bulk density were mainly driven by Ω_A (Random Forest, %IncMSE = 19.32 and 17.59, respectively), followed by pH (% IncMSE = 16.41 and 14.42, respectively) and temperature (%IncMSE = 13.70 and 14.08, respectively). PERMANOVA confirmed significant effects of pH ($p = 0.001$), its interaction with temperature ($p = 0.005$), and the three-way interaction ($p = 0.002$) on both variables. Temperature alone had no significant effect. This suggests that while individual environmental factors like pH and Ω_A significantly influence porosity and bulk density, the interactions among environmental drivers led to a synergistic effect, that amply skeletal degradation beyond additive predictions.

3.4. Shell mechanical properties

The following results refer to compression tests conducted under *dry* conditions, as no differences emerged under *wet* conditions (Fig. 3, Suppl. Table 6). Under dry compression conditions, fracture type distribution varied significantly among treatments (G-test, $p < 0.01$; Fig. 3d). Pairwise G-test with Holm correction revealed differences between $T1_{control}$ and $T8_{\downarrow pH\ \uparrow Temp\ \downarrow Sal}$ ($p = 0.038$), $T6_{\downarrow pH\ \uparrow Temp}$ ($p = 0.040$), and $T4_{\uparrow Temp\ \downarrow Sal}$ ($p = 0.041$), indicating that the control treatment showed a distinct fracture pattern compared to several combined stress conditions (Fig. 3d). Specifically, $T1_{control}$ was dominated by Type I

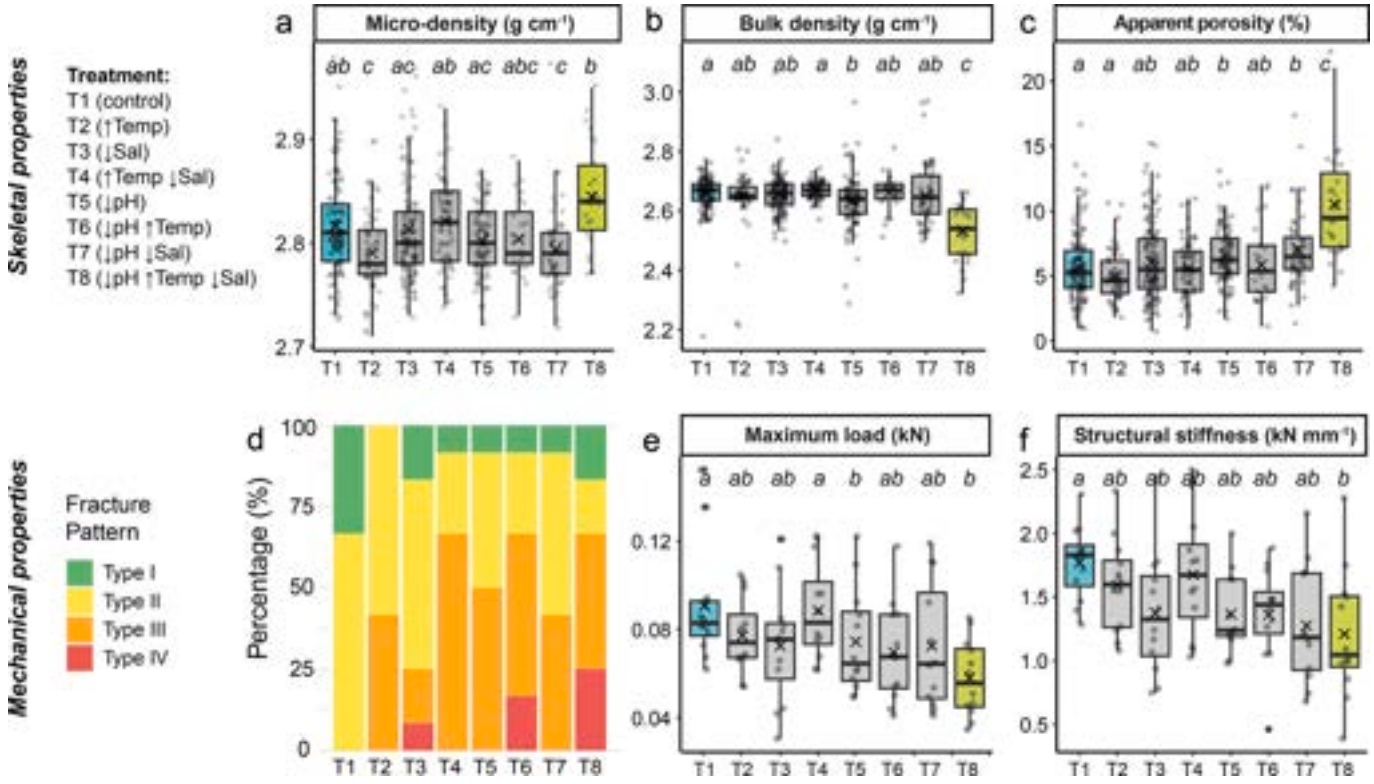

Fig. 3. Skeletal and mechanical properties across treatments (T1 to T8). a-c: Micro-density, bulk density, and apparent porosity. d: Percent distribution of fracture pattern types (Type I-IV). e-f: Maximum load and structural stiffness. Crosses represent mean values and different letters indicate statistically significant differences between treatments (Dunn's and Tukey's post-hoc test, $p \leq 0.05$). Light blue bars represent the control treatment (T1), while acid green bars indicate the three-factor combined condition (T8). (For interpretation of the references to colour in this figure legend, the reader is referred to the web version of this article.)

fractures (compact failure), while $T4_{\uparrow Temp+\downarrow Sal}$, $T6_{\downarrow pH\ \uparrow Temp}$, and $T8_{\downarrow pH\ \uparrow Temp\ \downarrow Sal}$ showed higher frequencies of more fragmented fracture types (Type III and IV), suggesting greater structural fragility under acidification and thermal-salinity stress (Fig. 3d). Mechanical properties under dry compression also varied significantly across treatments (K—W test and ANOVA, $p \leq 0.05$; Fig. 3, Suppl. Table 6). Maximum load decreased from 0.09 ± 0.02 kN in $T1_{control}$ to 0.06 ± 0.01 kN in $T8_{\downarrow pH\ \uparrow Temp\ \downarrow Sal}$, corresponding to 36% reduction under simultaneous pH, temperature, and salinity changes (Fig. 3e, Suppl. Table 6). Similarly, structural stiffness dropped by 32%, from 1.77 ± 0.19 kN mm^{-1} in T1 to 1.21 ± 0.32 kN mm^{-1} in $T8_{\downarrow pH\ \uparrow Temp\ \downarrow Sal}$ (Fig. 3f, Suppl. Table 6), indicating reduced shell rigidity with the three-factor combined stress exposure. PERMANOVA confirmed a significant effect of pH on both maximum load ($p = 0.007$) and stiffness ($p = 0.001$), with a significant three-way interaction (pH:T:S) for maximum load ($p = 0.043$). Random Forest analysis further supported the influence of chemical drivers, with Ω_A and pH being the top predictors of maximum load (%IncMSE = 12.8 and 8.6, respectively) and stiffness (%IncMSE = 13.6 and 12.3, respectively).

3.5. Shell microstructural properties

XRD and FTIR analyses confirmed that the clam shells were primarily composed of aragonite (Fig. 4). FTIR spectra showed characteristic absorption bands of aragonite (~1484 cm^{-1} for ν_3, ~859 cm^{-1} for ν_2, and ~ 712 cm^{-1} for ν_4; Fig. 4) with no detectable band shifts among treatments. XRD quantitative phase analysis revealed >98 wt% aragonite across treatments, with minor calcite content (0.38–1.98 wt%; Fig. 5, Suppl. Table 7). Significant differences in aragonite/calcite ratios were found (K—W test, $p \leq 0.05$) for whole-shell, but not for the umbo, ventral or central regions (Suppl. Table 8–9-10). Specifically, considering whole-shell samples, $T8_{\downarrow pH\ \uparrow Temp\ \downarrow Sal}$ exhibited the highest calcite content (1.98 wt%) and a slight aragonite decrease (98.02 wt%) compared to the $T1_{control}$ (0.50 and 99.50 wt%, respectively; Fig. 5, Suppl. Table 7). This trend, though not significant after post-hoc adjustment, was supported by PERMANOVA results showing a strong and significant interaction between the three environmental factors (pH:T:S, $p < 0.001$), indicating a synergistic effect of acidification, warming, and hyposalinity on mineralogical composition. Crystallite size along planes (111), (021), and (200) differed significantly across treatments for whole-shell (K—W test, $p \leq 0.05$; Fig. 5, Suppl. Table 7), but post-hoc tests failed to confirm pairwise differences after *p*-adjustment. The largest crystallites occurred in $T1_{control}$ and the smallest in $T8_{\downarrow pH\ \uparrow Temp\ \downarrow Sal}$, corresponding to a ~ 37% reduction (Fig. 5, Suppl. Table 7). Again, PERMANOVA confirmed a significant three-way interaction (pH:T:S, $p < 0.001$), supporting the presence of non-additive effects where combined stressors induced a more marked reduction in crystallite dimensions than individual factors. No differences emerged in crystallite size measurements of individual zones (umbo, central and edge; Suppl. Table 8–9-10). Intracrystalline material and shell decarbonation were homogeneous across treatments (Suppl. Table 11). ICP-OES analyses showed that Ca content ranged between 34 and 37 wt%, with significant reductions in $T7_{\downarrow pH\ \downarrow Sal}$ (34.17 ± 1.16 wt%) compared to $T1_{control}$ (37.20 ± 4.57 wt%) and $T3_{\downarrow Sal}$ (37.64 ± 2.17 wt%; Tukey's test, $p \leq 0.05$; Fig. 5, Suppl. Table 7), suggesting reduced calcium incorporation under combined acidification and hyposalinity stress. Although $T8_{\downarrow pH\ \uparrow Temp\ \downarrow Sal}$ exhibited high variance, removal of a single outlier aligned its Ca content with a consistent ~9% reduction trend under the three-factor combined stress (Fig. 5, Suppl. Table 7). PERMANOVA confirmed that pH had a significant effect ($p = 0.018$), and that the interaction between pH and temperature was also significant ($p = 0.002$). Random Forest analysis confirmed that microstructural and mineralogical responses (crystallite size, aragonite/calcite mineral ratio and Ca concentration) were primarily influenced by Ω_A and pH, with lower predictive contributions from temperature and salinity, highlighting the central role of carbonate system in driving early biomineral alterations.

4. Discussion

This study provides integrative experimental insight into the skeletal responses of *Chamelea gallina* to combined acidification, warming, and hyposalinity, highlighting early alterations in shell skeletal, mechanical, and microstructural properties during a short-term exposure in controlled aquaria. The sensitivity of this species to environmental changes, particularly warming and salinity fluctuations, has been previously documented along latitudinal gradients in the Adriatic Sea (Gizzi et al., 2016; Mancuso et al., 2023, 2019) and along the temporal gradient from the Holocene sedimentary record to present-day thanatocoenosis of the Po Plain–Adriatic system (Cheli et al., 2025, 2021). Moreover, although several studies have examined the physiological responses of *C. gallina* to environmental stressors (Matozzo et al., 2013,

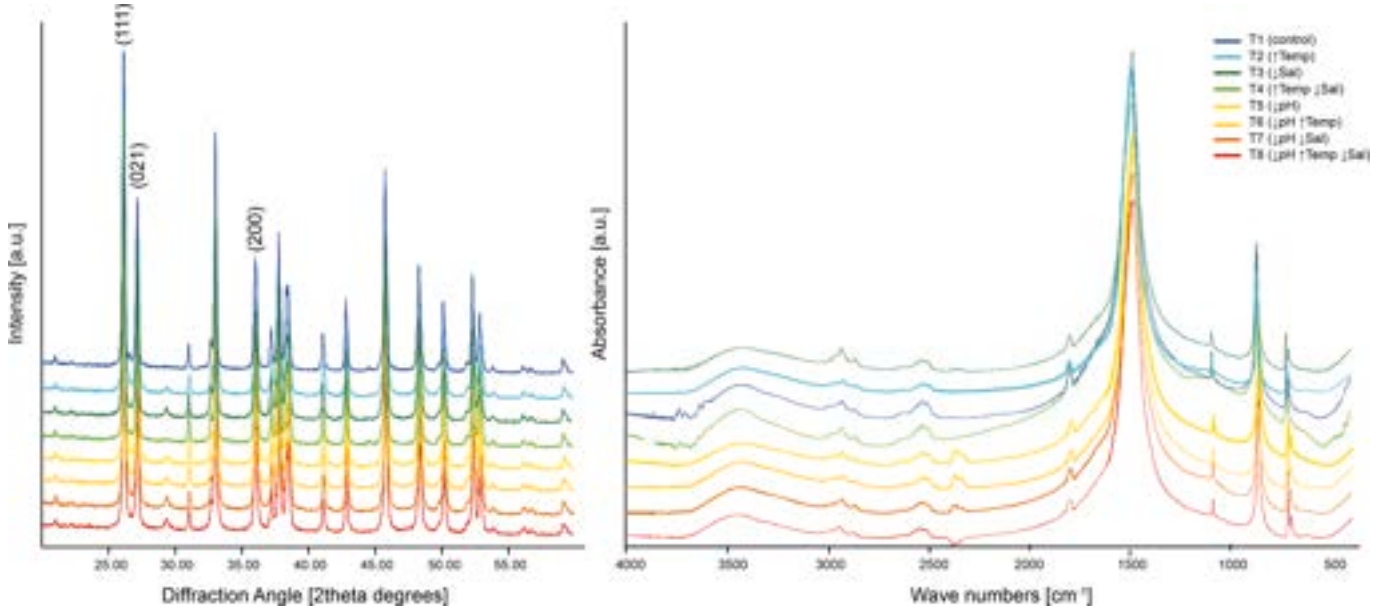

Fig. 4. XRD pattern and FTIR spectrum are shown for each treatment (T1-T8). All the XRD peaks were assigned to aragonite. Diffraction patterns are offset to increase readability.

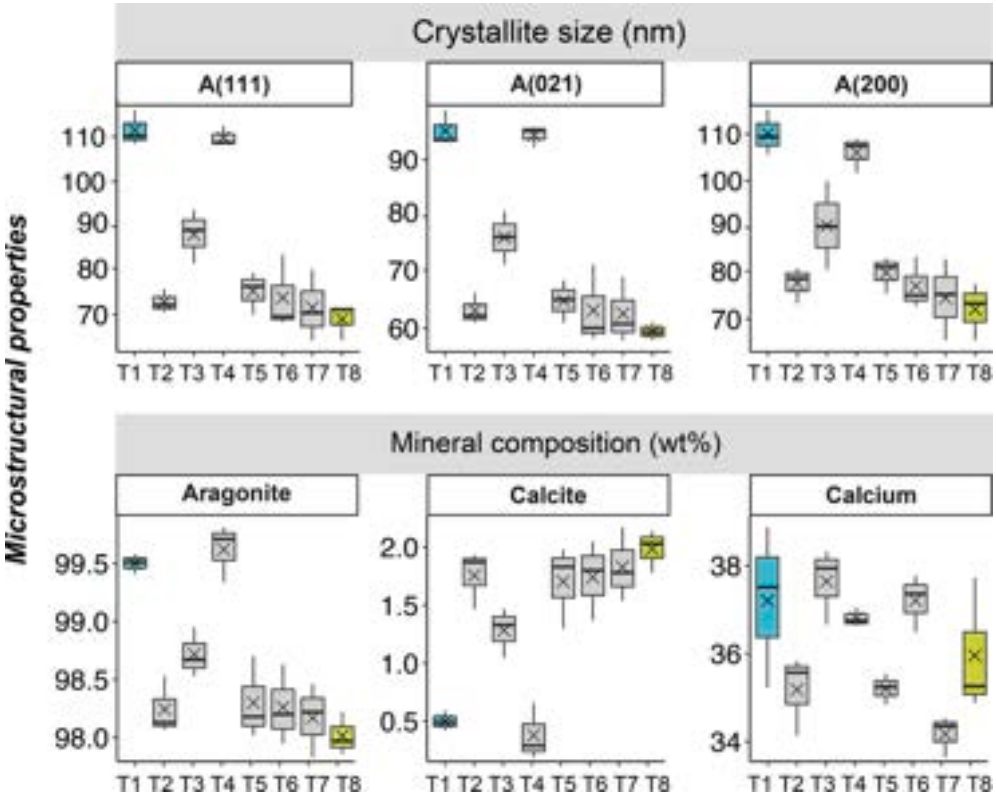

Fig. 5. Shell microstructural properties (crystallite size and mineral composition) across treatments (T1 to T8), obtained from XRD and ICP-OES analyses. $n = 3$ independent samples for each treatment. Crosses represent mean values. Light blue bars represent the control treatment (T1), while acid green bars indicate the three-factor combined condition (T8). (For interpretation of the references to colour in this figure legend, the reader is referred to the web version of this article.)

2012; Pilo et al., 2014), the influence of chemical drivers, such as pH and calcium carbonate saturation state (Ω_A), and their interaction with physical parameters remains poorly understood.

Commercial-sized clams with homogeneous shell length across treatments were used to minimize size-related bias and attribute observed changes in shell properties to environmental changes. At the end of the experiment, clams reared in reduced pH and raised temperature ($T6_{\downarrow pH\ \uparrow Temp}$ and $T8_{\downarrow pH\ \uparrow Temp\ \downarrow Sal}$) showed the higher mortality rate, supports the hypothesis that acidification and warming act as cumulative stressors affecting different physiological pathways (Krishna et al., 2025). The absence of a significant interaction between pH and temperature suggests an additive rather than synergistic effect, aligning with previous work on bivalves where temperature increases metabolic demand and acidification impairs calcification (Gestoso et al., 2016; Martel et al., 2022; Pilo et al., 2014; Rynkowski et al., 2025).

Although salinity alone did not cause significant mortality, its interaction with other stressors, particularly temperature, increased mortality rates, indicating its role as a modulating factor that can exacerbate physiological stress beyond compensatory limits (Bae et al., 2021; Dickinson et al., 2012; Rato et al., 2022; Yuan et al., 2016). A similar interaction has been observed in other bivalves, such as *Ruditapes decussatus* and *Venerupis philippinarum*, where clams exposed to extreme temperature and hyposalinity showed abrupt increases in mortality (Bae et al., 2021; Rato et al., 2022). These findings reinforce concerns that projected climate scenarios involving high temperatures and episodic freshwater inputs may jeopardize survival in coastal bivalve populations. Despite pronounced effects on survival, the condition index (CI) remained relatively stable across treatments, showing only minor differences and high within-group variability. As CI reflects the ratio of soft tissue to shell mass, it generally responds only to prolonged stress or sustained resource shifts, while short-term stress may elicit physiological changes not immediately evident at the whole-body level (Beaudry et al., 2016).

Shell macro and micro-scale properties seemed to be highly responsive to experimental conditions after only 21 days of exposure. Apparent porosity and bulk density emerged as the most sensitive indicators of skeletal change, both exhibiting a clear synergistic response, characterized by markedly elevated porosity (+92%) and reduced density (−5%) under combined acidification, warming, and hyposalinity. Micro-density, which reflects the density of calcium carbonate, showed weak variations, with a mean value of 2.8 g cm^{-3} in line with typical density of biogenic biologically produced aragonite, indicating conserved mineralogical characteristics. The observed skeletal weakening, characterized by increased porosity and reduced bulk density, likely compromised shell mechanical integrity, as confirmed by compression tests under dry conditions. Shells exposed to acidification, warming, and hyposalinity exhibited reduced maximum load and stiffness, indicating weaker and more fracture-prone shells. These effects emerged only under dry conditions, not when shells were hydrated, emphasizing the role of water and the organic matrix in maintaining structural resilience (Ji et al., 2020; Li et al., 2023; Neves and Mano, 2005). Hydration likely restores elasticity to the organic components (Ji et al., 2020), attenuating stress propagation (Barthelat et al., 2007; Kamat et al., 2000) and masking weaknesses induced by environmental stressors (Fitzer et al., 2014; Marin et al., 2012). Because the organic matrix constitutes only 0.1–5 wt% of shell mass (Marin et al., 2012), and averaged 1.8 wt% in *C. gallina* without variation among treatments, it cannot account for the observed mechanical differences. Increased fragility under dry conditions, instead, likely reflects cumulative calcification impairments at the macroscale (increased porosity) and microscale (modifications in crystallite size and mineral composition). Crystallite size was markedly reduced in shells exposed to combined low pH, elevated temperature, and reduced salinity (~ − 33–37%), suggesting early disruption of crystal growth and constrained crystal

maturation under stressful conditions. Although post-hoc comparisons did not retain statistical significance after correction, likely due to sample size and data variability, the consistent trend across planes and treatments pointed to the onset of a stress-driven response in shell organization. Similar microstructural changes have been reported in mollusks exposed to acidification, that have shown to produce smaller and less ordered crystals, and less compact microstructural assemblies, all factors that may reduce fracture resistance and overall structural performance (Fitzer et al., 2014, 2016; Hahn et al., 2011; Leung et al., 2017; Meng et al., 2018). Mineralogical analyses confirmed that *C. gallina* shells remained predominantly aragonitic across treatments, consistent with previous studies (Gizzi et al., 2016; Kocabaş et al., 2023; Mancuso et al., 2019). However, a slight increase in calcite content was detected under acidified conditions, reaching up to 1.98 wt% in $T8_{\downarrow pH \uparrow Temp \downarrow Sal}$. Although not statistically significant, the consistent trend observed across treatments suggested an emerging shift toward increased calcite precipitation or disrupted aragonite crystallization under ocean acidification. Comparable patterns in other bivalves and gastropods (Fitzer et al., 2014; Ries et al., 2009; Hahn et al., 2011), indicated that such changes often arise from localized polymorphic instability rather than complete phase transitions. These subtle mineralogical shifts likely signal early disruption of the biomineralization pathway, driven by reduced carbonate saturation (Ω_A) and altered ion availability under acidified conditions (Waldbusser and Salisbury, 2014).

Calcium content in *C. gallina* showed reduced values under low pH, especially in the combined acidification and hyposalinity condition ($T7_{\downarrow pH \downarrow Sal}$). Given that calcium concentrations in bivalve shells typically average around ~35 wt% (a value confirmed in this study), and accounts for 95–99% of the shell mineral mass (Schöne et al., 2010), calcium content serves as a reliable proxy for calcification efficiency (Frieder et al., 2017b). Its decline therefore points to an early limitation in calcium incorporation under multi-stressor conditions. Altogether, these findings may represent early signs of stress-induced limitations in shell formation processes which, if sustained over time, could compromise the calcification potential of *C. gallina* under chronic environmental stress.

This study provides compelling evidence that ocean acidification, warming, and hyposalinity jointly affect the shell of *C. gallina*, altering its structural, mechanical, and compositional properties even after short-term exposure. The combined action increased porosity, reduced bulk density, weaken mechanical resistance, decreased crystallite size, and lowered calcium incorporation, all early signatures of impaired calcification and reduced shell resilience. Many of the responses under the triple-stressor treatment (low pH, high temperature, low salinity) exceeded those expected from single-stressor impacts, suggesting synergistic interactions that amplify organismal vulnerability, a growing pattern among marine invertebrates (Przeslawski et al., 2015; Wu et al., 2018). These non-additive effects highlight the importance of multi-stressor experimental approaches to more accurate predict marine calcifiers' responses under realistic climate change scenarios. A limitation of this study is the relatively short exposure duration (21 days), which does not replicate the chronic nature of climate change. However, short-term mesocosm experiments are effective in identifying early responses and windows of vulnerability to rapid environmental fluctuations, which are common in coastal systems such as the Adriatic Sea. Accordingly, the observed responses should be interpreted as acute effects rather than long-term acclimation or adaptation. Future work should extend exposure durations, include additional life stages (e.g., juveniles), and apply mechanistic and modeling approaches to better resolve how multiple stressors interact to affect shell structure, mechanical properties, and survival of *C. gallina*.

The clear multi-scale weakening of *C. gallina* under combined stressors, may also compromise the shell's mechanical protection and increase vulnerability to durophagous predators (Amaral et al., 2012; Awad et al., 2023; Green et al., 2009). Given the ecological and economic relevance of *C. gallina* in the Adriatic Sea, reduced shell integrity could also lead to lower product quality and higher discard rates during fishing operations, with potential socio-economic implications (Bressan et al., 2014; Gizzi et al., 2016). This study underscores the value of a multi-scale approach, integrating structural and mineralogical responses, and offers a comprehensive perspective on how climate change may weaken the resilience of shell-forming species in coastal ecosystems. These insights are critical for assessing species vulnerability and supporting both biodiversity conservation and the sustainability of bivalve fisheries in an era of accelerating environmental change.

5. Conclusions

This study provides experimental evidence that combined exposure to ocean acidification, warming, and hyposalinity weakens the shell of *Chamelea gallina*, compromising shell integrity and increasing mortality even over short timescales. The observed increase in porosity and reduction in bulk density and mechanical resistance, together with subtle changes in shell mineralogy, indicate early impairment of calcification processes. Notably, several responses were stronger under combined stressors than under single-stressor conditions, highlighting the role of synergistic interactions in exacerbating skeletal weakening. Given the ecological and commercial importance of *C. gallina* in the Adriatic Sea, these findings suggest increased vulnerability of this species under future climate scenarios and emphasize the need for mitigation strategies to preserve coastal ecosystems and bivalve fisheries.

CRediT authorship contribution statement

Arianna Mancuso: Writing – review & editing, Writing – original draft, Visualization, Validation, Methodology, Investigation, Funding acquisition, Formal analysis, Data curation, Conceptualization. **Francesca Giovanna Bardone:** Writing – review & editing, Writing – original draft, Visualization, Validation, Methodology, Investigation, Formal analysis, Data curation. **Chiara Marchini:** Writing – review & editing, Methodology, Formal analysis. **Matilde Gironi:** Writing – review & editing, Formal analysis. **Anna Chiara Dalpozzo:** Writing – review & editing, Formal analysis. **Teresa Sani:** Writing – review & editing, Formal analysis. **Federico Girolametti:** Writing – review & editing, Formal analysis. **Anna Annibaldi:** Writing – review & editing, Resources, Formal analysis. **Francisco Arenas:** Writing – review & editing, Validation, Supervision, Resources, Methodology, Investigation, Conceptualization. **Giuseppe Falini:** Writing – review & editing, Validation, Supervision, Resources, Methodology, Conceptualization. **Stefano Goffredo:** Writing – review & editing, Validation, Supervision, Resources, Methodology, Data curation, Conceptualization.

Declaration of competing interest

The authors declare that they have no known competing financial interests or personal relationships that could have appeared to influence the work reported in this paper.

Acknowledgements

The research leading to these results has received funding from: 1) European Union's Horizon 2020 research and innovation program (Grant Agreement No. 730984) in the context of ASSEMBLE PLUS project., 2) the National Recovery and Resilience Plan (NRRP), Mission 4 Component 2 Investment 1.4 - Call for tender No. 3138 of 16 December 2021, rectified by Decree n.3175 of 18 December 2021 of Italian Ministry of University and Research funded by the European Union – NextGenerationEU. Project code CN_00000033, Concession Decree No. 1034 of 17 June 2022 adopted by the Italian Ministry of University and Research, CUP J33C22001190001, Project title “National Biodiversity Future Center - NBFC”.

This study represents partial fulfilment of the requirements for the doctoral thesis of Francesca Giovanna Bardone, within the international Program "Innovative Technologies and Sustainable Use of Mediterranean Sea Fishery and Biological Resources" (FishMed-PhD; www.FishMed-PhD.org) at the University of Bologna, Italy. Open access publishing facilitated by the University of Bologna, as part of the Wiley - CRUI-CARE agreement.

Appendix A. Supplementary data

Supplementary data to this article can be found online at https://doi.org/10.1016/j.marpolbul.2026.119304.

Data availability

Datasets generated and analyzed during the current study are available from the corresponding author on reasonable request.

References

Amaral, V., Cabral, H.N., Bishop, M.J., 2012. Effects of estuarine acidification on predator–prey interactions. Mar. Ecol. Prog. Ser. 445, 117–127.
Andersson, A.J., Mackenzie, F.T., Lerman, A., 2006. Coastal Ocean CO_2–carbonic acid–carbonate sediment system of the Anthropocene. Glob. Biogeochem. Cycles 20.
Awad, M.E., Madkour, F.F., Shaltout, N.A., Abu El-Regal, M., Elshazly, A., El-Wazzan, E., 2023. Sensitivity of the grooved carpet shell clam, *Ruditapes decussatus* (Linnaeus, 1758), to ocean acidification. Arab. J. Geosci. 16, 110.
Bae, H., Im, J., Joo, S., Cho, B., Kim, T., 2021. The effects of temperature and salinity stressors on the survival, condition and valve closure of the Manila clam, *Venerupis philippinarum* in a holding facility. J. Mar. Sci. Eng. 9, 754.
Barthelat, F., Tang, H., Zavattieri, P.D., Li, C.-M., Espinosa, H.D., 2007. On the mechanics of mother-of-pearl: a key feature in the material hierarchical structure. J. Mech. Phys. Solids 55, 306–337.
Beaudry, A., Fortier, M., Masson, S., Auffret, M., Brousseau, P., Fournier, M., 2016. Effect of temperature on immunocompetence of the blue mussel (*Mytilus edulis*). J Xenobiot 6, 5889.
Beniash, E., Ivanina, A., Lieb, N.S., Kurochkin, I., Sokolova, I.M., 2010. Elevated level of carbon dioxide affects metabolism and shell formation in oysters *Crassostrea virginica*. Mar. Ecol. Prog. Ser. 419, 95–108.
Bressan, M., Chinellato, A., Munari, M., Matozzo, V., Manci, A., Marčeta, T., Finos, L., Moro, I., Pastore, P., Badocco, D., 2014. Does seawater acidification affect survival, growth and shell integrity in bivalve juveniles? Mar. Environ. Res. 99, 136–148.
Cabral, J.P., Natal Jorge, R.M., 2007. Compressibility and shell failure in the European Atlantic *Patella* limpets. Mar. Biol. 150, 585–597.
Caroselli, E., Prada, F., Pasquini, L., Marzano, F.N., Zaccanti, F., Falini, G., Levy, O., Dubinsky, Z., Goffredo, S., 2011. Environmental implications of skeletal micro-density and porosity variation in two scleractinian corals. Zoology 114, 255–264.
Cheli, A., Mancuso, A., Azzarone, M., Fermani, S., Kaandorp, J., Marin, F., Montroni, D., Polishchuk, I., Prada, F., Stagioni, M., 2021. Climate variation during the Holocene influenced the skeletal properties of *Chamelea gallina* shells in the North Adriatic Sea (Italy). PLoS One 16, e0247590.
Cheli, A., Mancuso, A., Prada, F., Rojas, A., Falini, G., Goffredo, S., Scarponi, D., 2025. *Chamelea gallina* growth declined in the northern Adriatic Sea during the Holocene climate optimum. Sci. Rep. 15, 23353. https://doi.org/10.1038/s41598-025-07023-4.
Cossarini, G., Lazzari, P., Solidoro, C., 2015. Spatiotemporal variability of alkalinity in the Mediterranean Sea. Biogeosciences 12, 1647–1658.
Dickinson, G.H., Ivanina, A.V., Matoo, O.B., Pörtner, H.O., Lannig, G., Bock, C., Beniash, E., Sokolova, I.M., 2012. Interactive effects of salinity and elevated CO_2 levels on juvenile eastern oysters, *Crassostrea virginica*. J. Exp. Biol. 215, 29–43.
Doney, S.C., Busch, D.S., Cooley, S.R., Kroeker, K.J., 2020. The impacts of ocean acidification on marine ecosystems and reliant human communities. Annu. Rev. Environ. Resour. 45, 83–112.
FAO, 2023. The State of Mediterranean and Black Sea Fisheries 2023–Special Edition (General Fisheries Commission for the Mediterranean).
Feely, R.A., Doney, S.C., Cooley, S.R., 2009. Ocean acidification: present conditions and future changes in a high-CO_2 world. Oceanography 22, 36–47.
Feely, R.A., Jiang, L.-Q., Wanninkhof, R., Carter, B.R., Alin, S.R., Bednaršek, N., Cosca, C. E., 2023. Acidification of the global surface ocean. Oceanography 36, 120–129.
Fitzer, S.C., Phoenix, V.R., Cusack, M., Kamenos, N.A., 2014. Ocean acidification impacts mussel control on biomineralisation. Sci. Rep. 4, 6218.
Fitzer, S.C., Zhu, W., Tanner, K.E., Phoenix, V.R., Kamenos, N.A., Cusack, M., 2015. Ocean acidification alters the material properties of *Mytilus edulis* shells. J. R. Soc. Interface 12, 20141227.
Fitzer, S.C., Chung, P., Maccherozzi, F., Dhesi, S.S., Kamenos, N.A., Phoenix, V.R., Cusack, M., 2016. Biomineral shell formation under ocean acidification: a shift from order to chaos. Sci. Rep. 6, 21076.
Freeman, A.S., Byers, J.E., 2006. Divergent induced responses to an invasive predator in marine mussel populations. Science 1979 (313), 831–833.
Freitas, R., De Marchi, L., Bastos, M., Moreira, A., Velez, C., Chiesa, S., Wrona, F.J., Figueira, E., Soares, A.M.V.M., 2017. Effects of seawater acidification and salinity alterations on metabolic, osmoregulation and oxidative stress markers in *Mytilus galloprovincialis*. Ecol. Indic. 79, 54–62.
Frieder, C.A., Applebaum, S.L., Pan, T.-C.F., Hedgecock, D., Manahan, D.T., 2017a. Metabolic cost of calcification in bivalve larvae under experimental ocean acidification. ICES J. Mar. Sci. 74, 941–954.
Frieder, C.A., Applebaum, S.L., Pan, T.-C.F., Hedgecock, D., Manahan, D.T., 2017b. Metabolic cost of calcification in bivalve larvae under experimental ocean acidification. ICES J. Mar. Sci. 74, 941–954.
Gestoso, I., Arenas, F., Olabarria, C., 2016. Ecological interactions modulate responses of two intertidal mussel species to changes in temperature and pH. J. Exp. Mar. Biol. Ecol. 474, 116–125.
Giani, M., Ogrinc, N., Tamše, S., Cozzi, S., 2023. Elevated river inputs of the total alkalinity and dissolved inorganic carbon in the northern Adriatic Sea. Water (Basel) 15, 894.
Gizzi, F., Caccia, M.G., Simoncini, G.A., Mancuso, A., Reggi, M., Fermani, S., Brizi, L., Fantazzini, P., Stagioni, M., Falini, G., Piccinetti, C., Goffredo, S., 2016. Shell properties of commercial clam *Chamelea gallina* are influenced by temperature and solar radiation along a wide latitudinal gradient. Sci. Rep. 6, 1–12.
Grazioli, E., Guerranti, C., Pastorino, P., Esposito, G., Bianco, E., Simonetti, E., Rainis, S., Renzi, M., Terlizzi, A., 2022. Review of the scientific literature on biology, ecology, and aspects related to the fishing sector of the striped Venus (*Chamelea gallina*) in northern Adriatic Sea. J. Mar. Sci. Eng. 10, 1328.
Green, M.A., Waldbusser, G.G., Reilly, S.L., Emerson, K., O'Donnell, S., 2009. Death by dissolution: sediment saturation state as a mortality factor for juvenile bivalves. Limnol. Oceanogr. 54, 1037–1047.
Hahn, S., Rodolfo-Metalpa, R., Griesshaber, E., Schmahl, W.W., Buhl, D., Hall-Spencer, J. M., Baggini, C., Fehr, K.T., Immenhauser, A., 2011. Marine bivalve geochemistry and shell ultrastructure from modern low pH environments. Biogeosci. Discuss. 8, 10351.
Halpern, B.S., Frazier, M., Afflerbach, J., Lowndes, J.S., Micheli, F., O'Hara, C., Scarborough, C., Selkoe, K.A., 2019. Recent pace of change in human impact on the world's ocean. Sci. Rep. 9, 11609.
Harris, K.E., DeGrandpre, M.D., Hales, B., 2013. Aragonite saturation state dynamics in a coastal upwelling zone. Geophys. Res. Lett. 40, 2720–2725.
Ivanina, A.V., Dickinson, G.H., Matoo, O.B., Bagwe, R., Dickinson, A., Beniash, E., Sokolova, I.M., 2013. Interactive effects of elevated temperature and CO2 levels on energy metabolism and biomineralization of marine bivalves *Crassostrea virginica* and *Mercenaria mercenaria*. Comp. Biochem. Physiol. A Mol. Integr. Physiol. 166, 101–111.
Ji, H.M., Yang, W., Chen, D.L., Li, X.W., 2020. Natural arrangement of fiber-like aragonites and its impact on mechanical behavior of mollusk shells: a review. J. Mech. Behav. Biomed. Mater. 110, 103940.
Jiang, L.-Q., Kozyr, A., Relph, J.M., Ronje, E.I., Kamb, L., Burger, E., Myer, J., Nguyen, L., Arzayus, K.M., Boyer, T., 2023. The ocean carbon and acidification data system. Sci. Data 10, 136.
Kamat, S., Su, X., Ballarini, R., Heuer, A.H., 2000. Structural basis for the fracture toughness of the shell of the conch *Strombus gigas*. Nature 405, 1036–1040.
Kılıç, Ö., Belivermiş, M., Dere, B., Tillmann, A., Lannig, G., Bock, C., Sezer, N., Şahin, B., Demiralp, S., Bektaş, S., 2026. The multiple responses of *Mytilus galloprovincialis* in the multi-stressor scenario: impacts of low pH, low dissolved oxygen, and microplastics. Mar. Pollut. Bull. 222, 118875.
Kocabaş, F.K., Kocabaş, M., Çanakçi, A., Karabacak, A.H., 2023. Mechanical property and structural-elemental analysis of marine bivalve mollusc shells: *Cerastoderma edule, Chamelea gallina, Donax trunculus*. *Ruditapes decussatus*. Int Aquat Res 15, 39.
Krauzig, N., Coluccelli, A., Memmola, F., Penna, P., Moro, F., Zambianchi, E., Falco, P., 2025. Insights into exceptional freshening events in the northern Adriatic Sea throughout 2023-2024. State of the Planet Discussion Preprint.
Krishna, S., Lemmen, C., Örey, S., Rehren, J., Pane, J. Di, Mathis, M., Püts, M., Hokamp, S., Pradhan, H.K., Hasenbein, M., 2025. Interactive effects of multiple stressors in coastal ecosystems. Front. Mar. Sci. 11, 1481734.
Kristiansen, T., Butenschön, M., Peck, M.A., 2024. Statistically downscaled CMIP6 ocean variables for European waters. Sci. Rep. 14, 1209.
Kroeker, K.J., Kordas, R.L., Crim, R., Hendriks, I.E., Ramajo, L., Singh, G.S., Duarte, C.M., Gattuso, J., 2013. Impacts of ocean acidification on marine organisms: quantifying sensitivities and interaction with warming. Glob. Chang. Biol. 19, 1884–1896.
Lan, X., Tans, P., Thoning, K., 2023. NOAA Global Monitoring Laboratory. NOAA Greenhouse Gas Marine Boundary Layer Reference.
Lannig, G., Eilers, S., Pörtner, H.O., Sokolova, I.M., Bock, C., 2010. Impact of ocean acidification on energy metabolism of oyster, *Crassostrea gigas* - changes in metabolic pathways and thermal response. Mar. Drugs 8, 2318–2339.
Lee, H., Calvin, K., Dasgupta, D., Krinmer, G., Mukherji, A., Thorne, P., Trisos, C., Romero, J., Aldunce, P., Barret, K., 2023. Synthesis Report of the IPCC Sixth Assessment Report (AR6). Longer report, IPCC.
Lejeusne, C., Chevaldonné, P., Pergent-Martini, C., Boudouresque, C.F., Pérez, T., 2010. Climate change effects on a miniature ocean: the highly diverse, highly impacted Mediterranean Sea. Trends Ecol. Evol. 25, 250–260.
Leung, J.Y.S., Connell, S.D., Nagelkerken, I., Russell, B.D., 2017. Impacts of near-future ocean acidification and warming on the shell mechanical and geochemical properties of gastropods from intertidal to subtidal zones. Environ. Sci. Technol. 51, 12097–12103.
Li, S., Huang, J., Liu, C., Liu, Y., Zheng, G., Xie, L., Zhang, R., 2016. Interactive Effects of Seawater Acidification and Elevated Temperature on the Transcriptome and Biomineralization in the Pearl Oyster *Pinctada Fucata*. Environ Sci Technol SI.

Li, Y., Liang, S., Ji, H., Li, X., 2023. Effect of organic matrix viscoelasticity on indentation recovery behavior in a crossed-lamellar structure of mollusk shell. Mater. Lett. 330, 133391.
Liu, M., Guo, X., Han, L., Zhao, Y., Ge, C., 2026. Effects of ocean acidification on intestinal homeostasis and organismal performance in a marine bivalve: from microbial shifts to physiological suppression. Mar. Pollut. Bull. 222, 118704.
Lowenstam, H.A., Weiner, S., 1989. On biomineralization. Oxford University Press.
Mahapatra, S., Maity, J., Mandal, S., 2025. Assessing the physiological and oxidative stress status of *Etroplus suratensis* under elevated temperature and ocean acidification. Sci. Total Environ. 998, 180294.
Mancuso, A., Stagioni, M., Prada, F., Scarponi, D., Piccinetti, C., Goffredo, S., 2019. Environmental influence on calcification of the bivalve *Chamelea gallina* along a latitudinal gradient in the Adriatic Sea. Sci. Rep. 9, 11198.
Mancuso, A., Yam, R., Prada, F., Stagioni, M., Goffredo, S., Shemesh, A., 2023. Oxygen and carbon isotope variations in *Chamelea gallina* shells: environmental influences and vital effects. Geobiology 21, 119–132.
Marin, F., Le Roy, N., Marie, B., 2012. The formation and mineralization of mollusk shell. Front. Biosci. S4, 1099–1125.
Martel, S.I., Fernández, C., Lagos, N.A., Labra, F.A., Duarte, C., Vivanco, J.F., García-Herrera, C., Lardies, M.A., 2022. Acidification and high-temperature impacts on energetics and shell production of the edible clam *Ameghinomya antiqua*. Front. Mar. Sci. 9, 972135.
Matoo, O.B., Lannig, G., Bock, C., Sokolova, I.M., 2021. Temperature but not ocean acidification affects energy metabolism and enzyme activities in the blue mussel, *Mytilus edulis*. Ecol. Evol. 11, 3366–3379.
Matozzo, V., Chinellato, A., Munari, M., Finos, L., Bressan, M., Marin, G., 2012. First evidence of immunomodulation in bivalves under seawater acidification and increased temperature. PLoS One 7, 1–14.
Matozzo, V., Chinellato, A., Munari, M., Bressan, M., Marin, M.G., 2013. Can the combination of decreased pH and increased temperature values induce oxidative stress in the clam *Chamelea gallina* and the mussel *Mytilus galloprovincialis* ? Mar. Pollut. Bull. 72, 34–40.
Meng, Y., Guo, Z., Fitzer, S.C., Upadhyay, A., Chan, V., Li, C., Cusack, M., Yao, H., Yeung, K.W.K., Thiyagarajan, V., 2018. Ocean acidification reduces hardness and stiffness of the Portuguese oyster shell with impaired microstructure: a hierarchical analysis. Biogeosciences 15, 6833–6846.
Meng, Z.-J., Chen, C.-Z., Ma, Y.-Q., Feng, J.-X., Liu, L., Li, P., Li, Z.-H., 2026. Impacts of acidification and warming on carbon sequestration capacity in Pacific oysters: roles of biosynthesis and biodeposition. Aquac 610, 742906.
Nakamura, J., Ishida, M., 2025. Global warming and CO_2 emissions, in: blueprint for a methanol society: toward carbon-neutrality. Springer 3–26.
Neves, N.M., Mano, J.F., 2005. Structure/mechanical behavior relationships in crossed-lamellar sea shells. Mater. Sci. Eng. C 25, 113–118.
Nienhuis, S., Palmer, A.R., Harley, C.D.G., 2010. Elevated CO_2 affects shell dissolution rate but not calcification rate in a marine snail. Proc. R. Soc. B 277, 2553–2558.
Pilo, D., Range, P., Munari, M., Menif, N.T. El, Dellali, M., 2014. Impacts of CO_2 -induced seawater acidification on coastal Mediterranean bivalves and interactions with other climatic stressors. Reg environ. Change 14.
Posit team, 2025. RStudio: Integrated Development Environment for R.
Przeslawski, R., Byrne, M., Mellin, C., 2015. A review and meta-analysis of the effects of multiple abiotic stressors on marine embryos and larvae. Glob. Chang. Biol. 21, 2122–2140.
R Core Team, 2024. R: A language and environment for statistical computing.
Rahman, M.A., Henderson, S., Miller-Ezzy, P., Li, X.X., Qin, J.G., 2019. Immune response to temperature stress in three bivalve species: Pacific oyster *Crassostrea gigas*, Mediterranean mussel *Mytilus galloprovincialis* and mud cockle *Katelysia rhytiphora*. Fish Shellfish Immunol. 86, 868–874.
Rato, A., Joaquim, S., Matias, A.M., Roque, C., Marques, A., Matias, D., 2022. The impact of climate change on bivalve farming: combined effect of temperature and salinity on survival and feeding behavior of clams *Ruditapes decussatus*. Front. Mar. Sci. 9, 932310.
Ricci, F., Capellacci, S., Casabianca, S., Grilli, F., Campanelli, A., Marini, M., Penna, A., 2024. Variability of hydrographic and biogeochemical properties in the North-western Adriatic coastal waters in relation to river discharge and climate changes. Chemosphere 361, 142486.
Ries, J.B., Cohen, A.L., McCorkle, D.C., 2009. Marine calcifiers exhibit mixed responses to CO_2-induced ocean acidification. Geology 37, 1131–1134.
Romanelli, M., Cordisco, C.A., Giovanardi, O., 2009. The long-term decline of the *Chamelea gallina* L. (Bivalvia : Veneridae) clam fishery in the Adriatic Sea : is a synthesis possible ? Acta Adriat. 50 (2), 171–205.
Rynkowski, L., Ellis, J.I., Needham, H.R., Pilditch, C.A., 2025. A systematic review and meta-analysis of the cumulative effects of multiple stressors on marine bivalves. Mar. Biol. 172, 96.
Sanders, T., Schmittmann, L., Nascimento-Schulze, J.C., Melzner, F., 2018. High calcification costs limit mussel growth at low salinity. Front. Mar. Sci. 5, 352.
Sarazin, G., Michard, G., Prevot, F., 1999. A rapid and accurate spectroscopic method for alkalinity measurements in sea water samples. Water Res. 33, 290–294.
Schöne, B.R., Zhang, Z., Jacob, D., Gillikin, D.P., Tütken, T., Garbe-Schönberg, D., McConnaughey, T., Soldati, A., 2010. Effect of organic matrices on the determination of the trace element chemistry (Mg, Sr, Mg/ca, Sr/ca) of aragonitic bivalve shells (*Arctica islandica*) - comparison of ICP-OES and LA-ICP-MS data. Geochem. J. 44, 23–37.
Shirayama, Y., Thornton, H., 2005. Effect of increased atmospheric CO_2 on shallow water marine benthos. J Geophys Res Oceans 110.
Siedlecki, S.A., Pilcher, D.J., Hermann, A.J., Coyle, K., Mathis, J., 2017. The importance of freshwater to spatial variability of aragonite saturation state in the Gulf of Alaska. J Geophys Res Oceans 122, 8482–8502.
Sordo, L., Duarte, C., Joaquim, S., Gaspar, M.B., Matias, D., 2021. Long-term effects of high CO_2 on growth and survival of juveniles of the striped venus clam *Chamelea gallina*: implications of seawater carbonate chemistry. Mar. Biol. 168, 123.
Sordo, L., Esteves, E., Valente, J.F.A., Aníbal, J., Duarte, C., Alves, N., Baptista, T., Gaspar, M.B., 2024. Ocean acidification will not affect the shell strength of juveniles of the commercial clam species *Chamelea gallina*: implications of the local alkalinization of seawater. Mar. Environ. Res. 202, 106746.
Urbini, L., Ingrosso, G., Djakovac, T., Piacentino, S., Giani, M., 2020. Temporal and spatial variability of the CO_2 system in a riverine influenced area of the Mediterranean Sea, the northern Adriatic. Front. Mar. Sci. 7, 679.
Verri, G., Furnari, L., Gunduz, M., Senatore, A., Santos da Costa, V., De Lorenzis, A., Pinardi, N., 2024. Climate projections of the Adriatic Sea: role of river release. Front. Clim. 6, 1368413.
Waldbusser, G.G., Salisbury, J.E., 2014. Ocean acidification in the coastal zone from an organism's perspective: multiple system parameters, frequency domains, and habitats. Annu. Rev. Mar. Sci. 6, 221–247.
Walne, P.R., 1976. Experiments on the culture in the sea of the butterfish *Venerupis decussata* L. Aquac 8, 371–381.
Wu, F., Xie, Z., Lan, Y., Dupont, S., Sun, M., Cui, S., Huang, X., Huang, W., Liu, L., Hu, M., 2018. Short-term exposure of *Mytilus coruscus* to decreased pH and salinity change impacts immune parameters of their haemocytes. Front. Physiol. 9, 166.
Yuan, W.S., Walters, L.J., Brodsky, S.A., Schneider, K.R., Hoffman, E.A., 2016. Synergistic effects of salinity and temperature on the survival of two nonnative bivalve molluscs, *Perna viridis* (Linnaeus 1758) and *Mytella charruana* (d'Orbigny 1846). J. Mar. Sci. 2016, 9261309.
Zhao, X., Shi, W., Han, Y., Liu, S., Guo, C., Fu, W., Chai, X., Liu, G., 2017. Ocean acidification adversely influences metabolism, extracellular pH and calcification of an economically important marine bivalve, *Tegillarca granosa*. Mar. Environ. Res. 125, 82–89.
Zittis, G., Hadjinicolaou, P., Klangidou, M., Proestos, Y., Lelieveld, J., 2019. A multi-model, multi-scenario, and multi-domain analysis of regional climate projections for the Mediterranean. Reg. Environ. Change 19, 2621–2635.